Ground- and excited-states reactivity dynamics of hydrogen and helium atoms

ARTICLE *in* INTERNATIONAL JOURNAL OF QUANTUM CHEMISTRY · FEBRUARY 2003

Impact Factor: 1.43 · DOI: 10.1002/qua.10486

2 AUTHORS, INCLUDING:

Utpal Sarkar
Assam University
54 PUBLICATIONS **1,480** CITATIONS

SEE PROFILE

Ground- and Excited-States Reactivity Dynamics of Hydrogen and Helium Atoms

P. K. CHATTARAJ, U. SARKAR

Department of Chemistry, Indian Institute of Technology, Kharagpur 721 302, India

Received 27 January 2002; accepted 26 July 2002

DOI 10.1002/qua.10486

ABSTRACT: Dynamic profiles of various reactivity parameters like hardness, chemical potential, polarizability, phase volume, and electrophilicity index are studied in gaining insights into the ground- ($n = 1$) and excited- ($n = 15$) states dynamics of hydrogen and helium atoms. Pertinent time-dependent Schrödinger equations are solved for the ground and excited states of hydrogen atom and the Rydberg state of the helium atom while a generalized nonlinear Schrödinger equation is solved for the ground state of the helium atom, all interacting with external electric fields of different frequencies and intensities. For both the atoms ground states are more stable than the corresponding excited states. Hardness and phase volume can be used as diagnostics for the chaotic ionization from the Rydberg states of those atoms. Other quantities like higher-order harmonics also lend additional support. Dynamic variants of the maximum hardness and minimum polarizability principles are found to be operative.

Key words: density functional theory; chemical reactivity parameters; maximum hardness principle; minimum polarizability principle; electrophilicity

1. Introduction

Highly excited atoms in an external field has been an important research area [1–5] for both theoreticians and experimentalists. It has been shown [1] that a Rydberg atom in an external field exhibits many interesting phenomena depending on the amplitude and frequency of the external field. Experiments have been performed to show [2–4] that there is no ionization of the atom until a particular field strength, called critical field strength or threshold field amplitude, has been applied to it. The ionization curves of hydrogen and helium are different. In case of hydrogen atom, once the threshold is achieved the ionization increases monotonically and drastically with the increase of the field amplitude until it is fully ionized, but the ionization curve of helium can be thought of

Correspondence to: P. K. Chattaraj; e-mail: *pkc@chem.iitkgp.ernet.in*

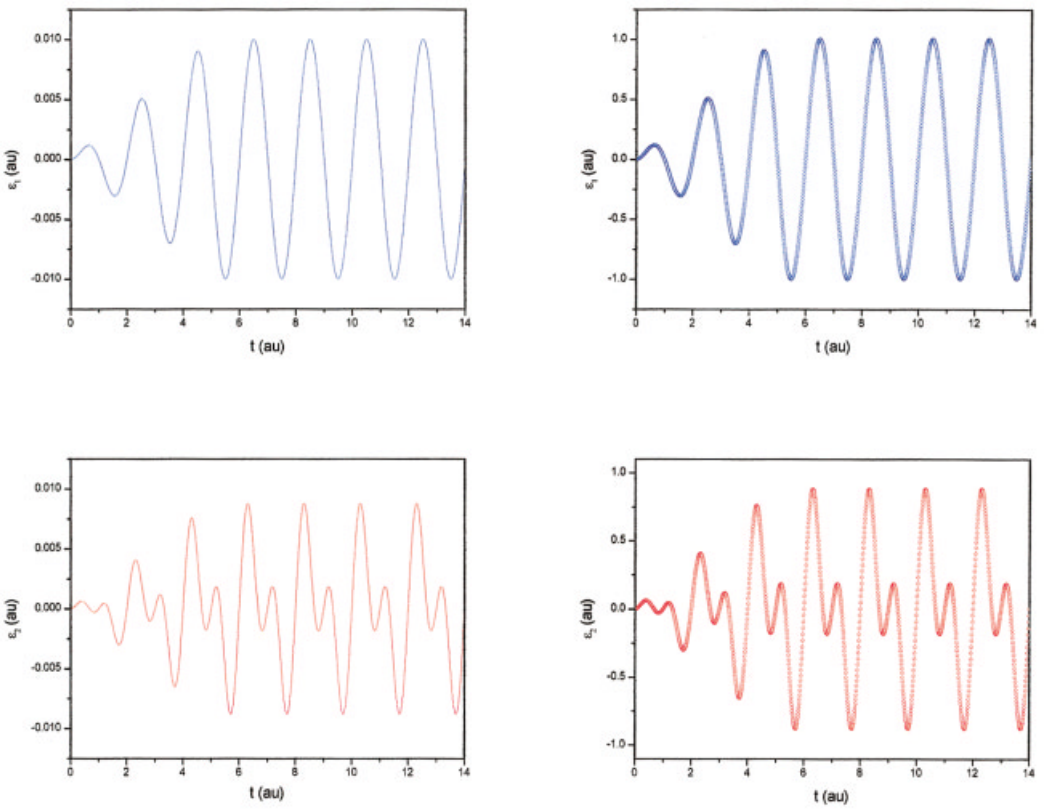

FIGURE 1. Time evolution of the external electric field: $\varepsilon 1$ (——), monochromatic pulse; $\varepsilon 2$ (—⊙—), bichromatic pulse. Maximum amplitudes (ε_0) = (blue rule) 0.01 a.u. (intensity = 3.509×10^{12} W/cm^2); (red rule) = 1 a.u. (intensity = 3.509×10^{16} W/cm^2), $t' = (5\pi/\omega_0)$, $\omega_0 = \pi$, $\omega_1 = 2\omega_0$.

as a series of two (or more) steps with stable plateaus between each successive threshold. The classical chaotic ionization of Rydberg helium atom takes place [5] at much lower field than the Rydberg hydrogen atom with same principal quantum number n, although the field required for complete ionization of helium is more than that of hydrogen. Hydrogen differs from helium mainly due to the non-Coulombic core potential of the latter.

In density functional theory (DFT) [6], there are many reactivity parameters with the help of which the structure, reactivity, and dynamics of a many-electron system can be described. Electronegativity, hardness, polarizability, phase volume, etc. are such parameters. Electronegativity [7] is the power of an atom in a molecule to attract electrons to itself whereas hardness [8] is defined through hard–soft acid-base (HSAB) principle of Pearson [9]. HSAB principle states that "hard likes hard and soft likes soft in an acid base reaction." For an N-electron system with total energy E, the quantitative definitions of electronegativity [10] and hardness [11] are, respectively, given by

$$\chi = -\mu = -\left(\frac{\partial E}{\partial N}\right)_{v(\vec{r})} \tag{1}$$

and

$$\eta = \frac{1}{2}\left(\frac{\partial^2 E}{\partial N^2}\right)_{v(\vec{r})} = \frac{1}{2}\left(\frac{\partial \mu}{\partial N}\right)_{v(\vec{r})}, \tag{2}$$

where μ and $v(\vec{r})$ are chemical potential and external potential, respectively.

Hardness is also defined [12] by the expression

$$\eta = \frac{1}{N}\int\int \eta(\vec{r}, \vec{r}')f(\vec{r}')\rho(\vec{r})d\vec{r}d\vec{r}', \tag{3}$$

where $f(\vec{r})$ is the Fukui function [13] and $\eta(\vec{r}, \vec{r}')$ is the hardness kernel. The hardness kernel is defined as [12]

$$\eta(\vec{r}, \vec{r}') = \frac{1}{2}\frac{\delta^2 F[\rho]}{\delta\rho(\vec{r})\delta\rho(\vec{r}')}, \tag{4}$$

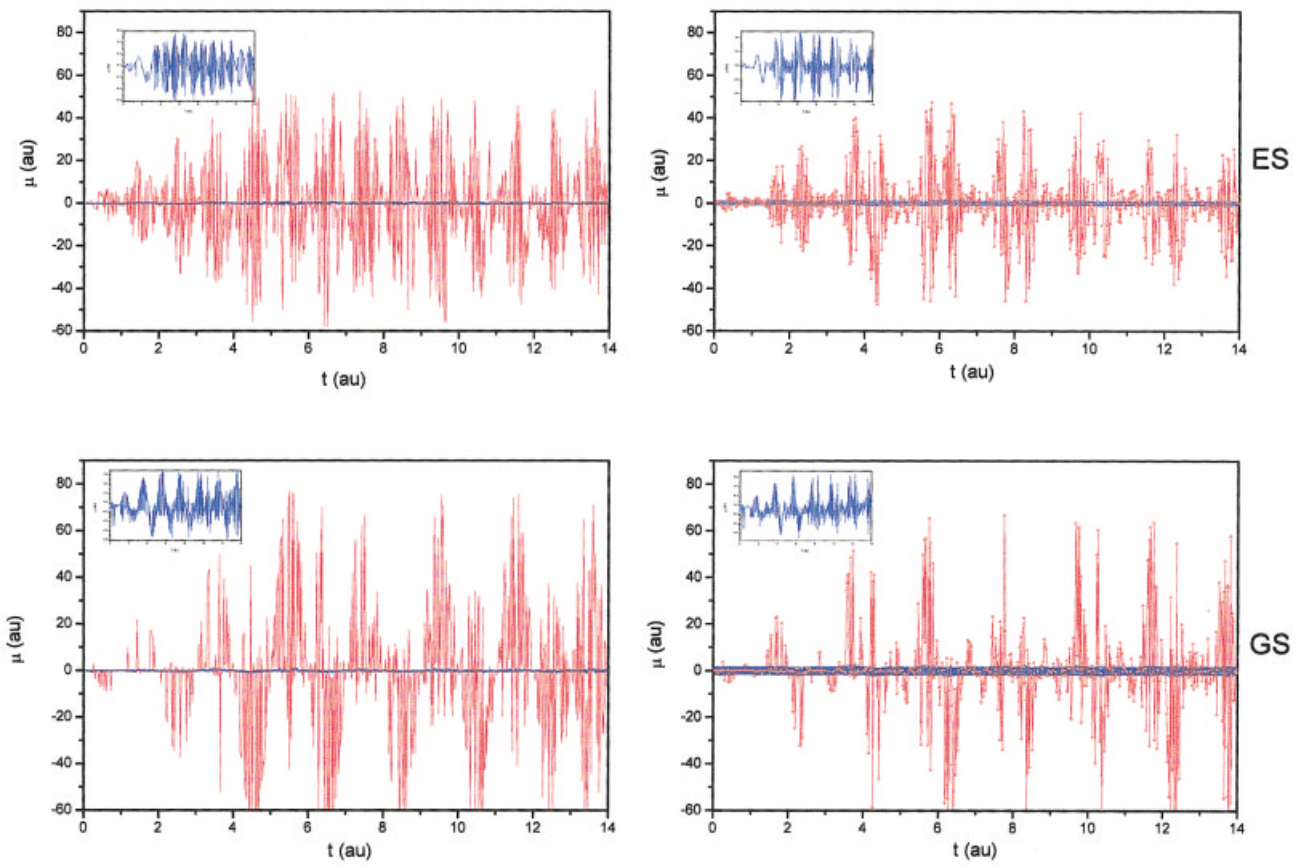

FIGURE 2. Time evolution of chemical potential (μ, a.u.) when a hydrogen atom is subjected to external electric fields (GS, ground state; ES, excited state): (——), monochromatic pulse; (—⊙—), bichromatic pulse. Maximum amplitudes (ε_0) = (blue rule) 0.01 a.u. (intensity = 3.509×10^{12} W/cm^2); (red rule) 1 a.u. (intensity = 3.509×10^{16} W/cm^2), $t' = (5\pi/\omega_0)$, $\omega_0 = \pi$, $\omega_1 = 2\omega_0$.

where $F[\rho]$ is the Hohenberg–Kohn universal functional of DFT [6]. The maximum hardness principle (MHP) [14] states that, "there seems to be a rule of nature that molecules arrange themselves so as to be as hard as possible," and Sanderson's [15] principle states that, "electronegativity of all atoms in a molecule are same." Chattaraj and Sengupta [16] have shown that if a system goes from a regular to a chaotic region then hardness (η value) often decreases.

To characterize an N-particle system completely under the influence of an external potential $v(\vec{r})$ one has to know N and $v(\vec{r})$. The response of the system by changing N at fixed $v(\vec{r})$ is given by χ and η whereas the response of the system by changing $v(\vec{r})$ at constant N is given by linear response function. Polarizability is an example of this type of response for a weak electric field. In DFT a stable system is associated with maximum hardness [14] and minimum polarizability [17–20]. A minimum polarizability principle (MPP) [17] states that, "a stable configuration is associated with minimum polarizability." In the present work we study the time evolution of various reactivity parameters for hydrogen and helium atoms in their ground and highly excited states in the presence of external fields of varying intensities and frequencies. In Section 2 we provide the theoretical background and in Section 3 numerical details are given. Section 4 contains results and discussion and Section 5 presents some concluding remarks.

2. Theoretical Background

Here, we study the dynamics of the ground state ($n = 1$) and a highly excited state ($n = 15$) of hydrogen and helium atoms placed in an oscillating electric field.

The pertinent time-dependent Schrödinger equation (TDSE, in a.u.) is given by

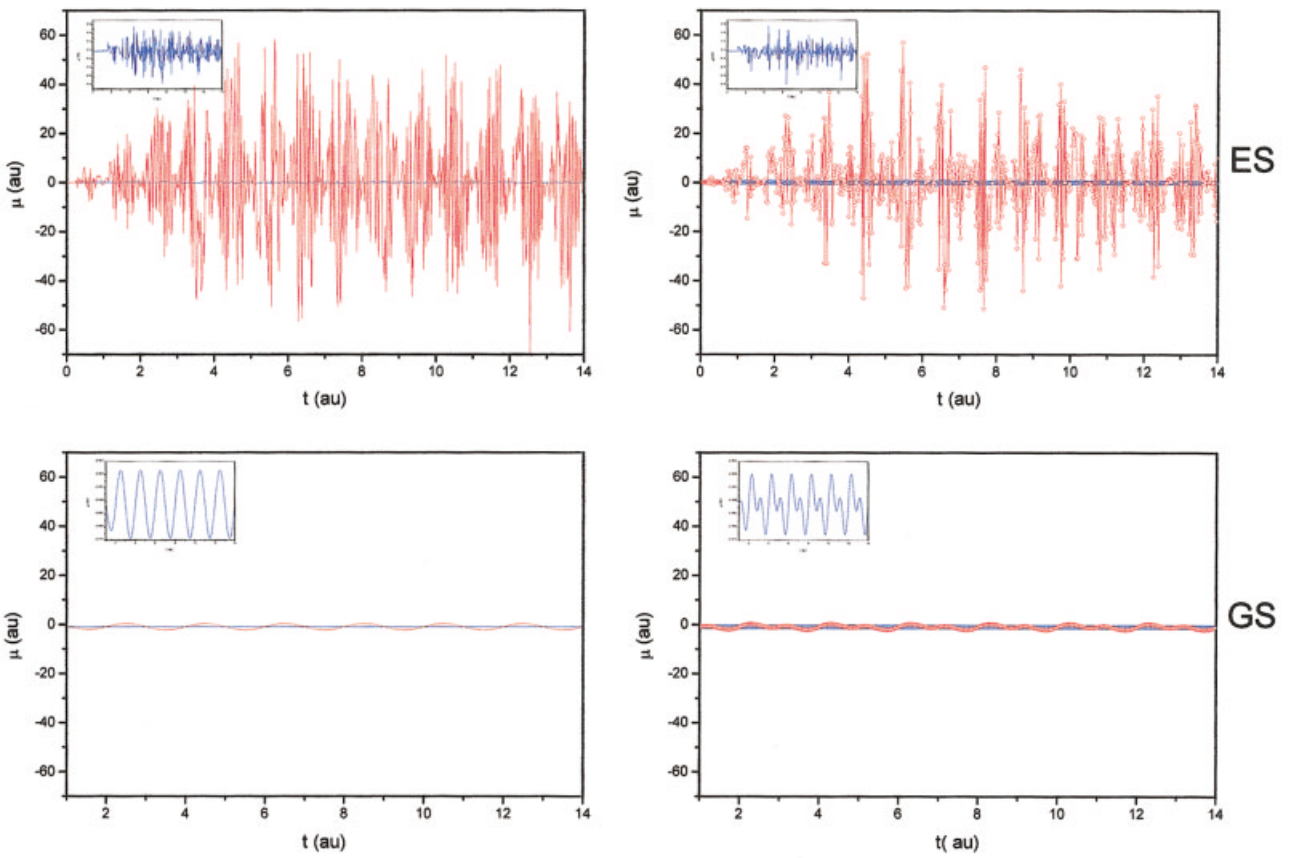

FIGURE 3. Time evolution of chemical potential (μ, a.u.) when a helium atom is subjected to external electric fields (GS, ground state; ES, excited state): (——), monochromatic pulse; (—⊙—), bichromatic pulse. Maximum amplitudes (ε_0) = (blue rule) 0.01 a.u. (intensity = 3.509×10^{12} W/cm^2); (red rule) 1 a.u. (intensity = 3.509×10^{16} W/cm^2), t' = $(5\pi/\omega_0)$, $\omega_0 = \pi$, $\omega_1 = 2\omega_0$.

$$\left[-\frac{1}{2}\nabla^2 + v1_{\text{core}}(\vec{r}) + v_{\text{ext}}(\vec{r}, t)\right]\psi(\vec{r}, t) = i\frac{\partial\psi(\vec{r}, t)}{\partial t}; \quad i = \sqrt{-1}, \quad (5)$$

where $v1_{\text{core}}(\vec{r}) = -(1/r)$ for the ground and excited states of hydrogen atom and $= v_n(\vec{r}) + v_s(\vec{r}) + v_p(\vec{r})$ for the excited state of helium atom. Here, $v_n(\vec{r}) = -(2/r)$ is the Coulomb potential between the unshielded helium nucleus and the Rydberg electron, $v_s(\vec{r}) = (1/r)(1 - (1 + 2r)e^{-4r})$ is the potential [5] due to shielding, which is the work done in moving the Rydberg electron from infinity to a point $\vec{r}$ through the charge probability cloud associated with the inner unperturbed 1s electron, and

$$v_p(\vec{r}) = -\frac{9}{64r^4}\left(1 - \left(1 + 4r + 24r^2 + \frac{160}{3}r^3 + \frac{64}{3}r^4\right)\frac{e^{-4r}}{3} - \frac{2}{3}(1 + 2r)^4 e^{-8r}\right)$$

is the core polarization, which is the correlation to $v_s(\vec{r})$ due to distortion [21] in the 1s wave function of the core electron by the Rydberg electron.

The external potential for the electric field polarized in z-direction may be written as (in dipole approximation and length gauge [5, 22])

$$v_{\text{ext}}(\vec{r}) = \varepsilon 1z, \text{ for a monochromatic pulse} \quad (6a)$$

$$= \varepsilon 2z, \text{ for a bichromatic pulse,} \quad (6b)$$

where

$$\varepsilon 1 = \varepsilon \sin(\omega_0 t) \quad (6c)$$

and

$$\varepsilon 2 = 0.5\varepsilon[\sin(\omega_0 t) + \sin(\omega_1 t)]. \quad (6d)$$

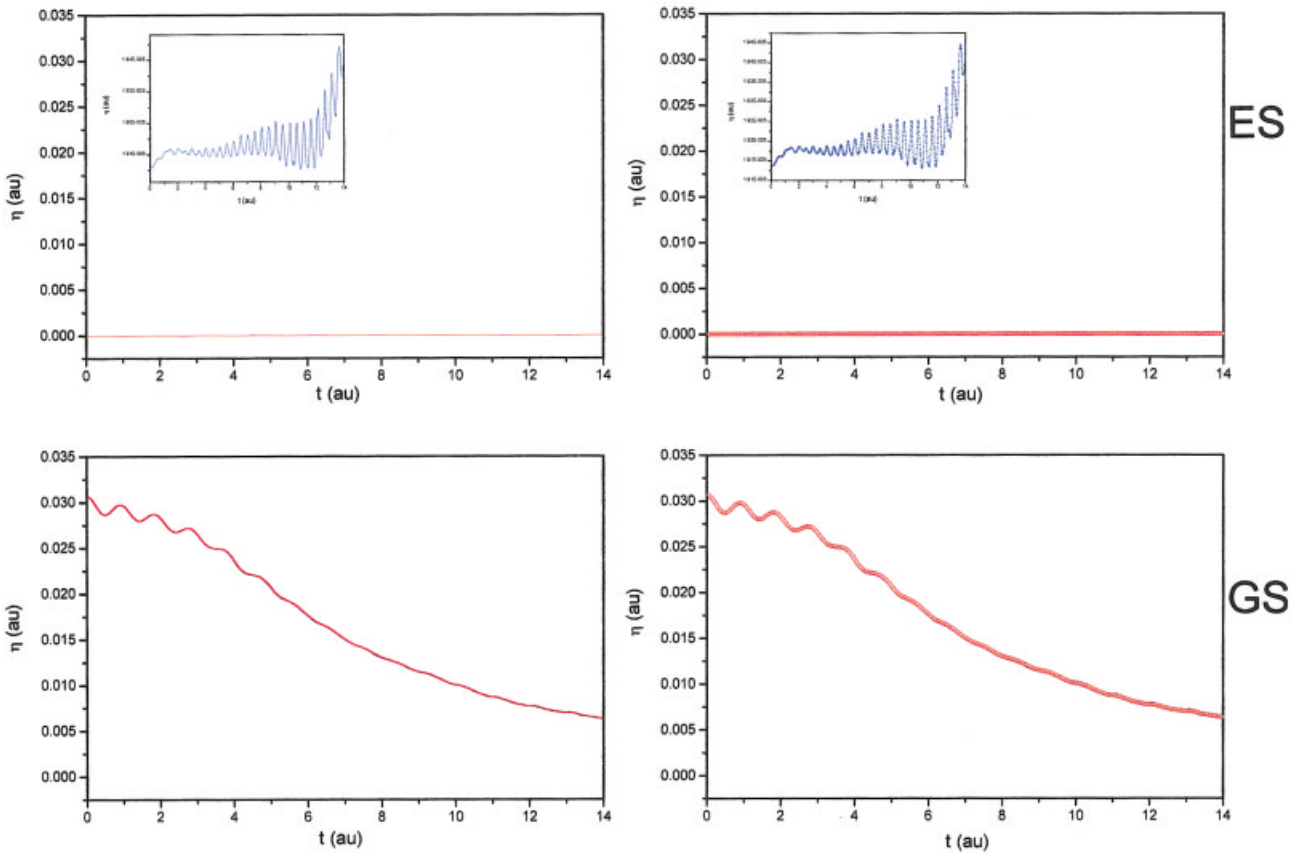

FIGURE 4. Time evolution of chemical hardness (η, a.u.) when a hydrogen atom is subjected to external electric fields. See the caption of Fig. 2 for details.

Because the field is z-polarized the angular momentum component along this axis is conserved [5] and the use of sinusoidal pulse guarantees that the initial condition would correspond to the atom in the absence of the field [22]. We have excluded the magnetic force, which is originating from the variation of the electric field, because its amplitude (ε/c, c is the velocity of light) is low. To have a slow oscillation during and after the electric field being switched on, ε is written in terms of the maximum amplitude ε_0 and the switch-on time t' as

$$\varepsilon = \varepsilon_0 \frac{t}{t'} \quad \text{for } 0 \le t \le t' \tag{7a}$$

$$= \varepsilon_0 \quad \text{otherwise.} \tag{7b}$$

The linear ramp used here allows the intensity to increase linearly and slowly so that the classical action is conserved and the intensity increase is adiabatic during the switch-on time of the laser [5, 22].

In the time-dependent DFT (TDDFT) [23], all dynamic properties of a system are functionals of charge density $\rho(\vec{r}, t)$ and current density $\vec{j}(\vec{r}, t)$. The dynamics of a many-particle system under some external potential may be studied by two quantum fluid dynamic (QFD) equations, viz., an equation of continuity,

$$\frac{\partial \rho(\vec{r}, t)}{\partial t} = -\nabla \cdot \vec{j}(\vec{r}, t) \tag{8a}$$

and a Euler-type equation of motion,

$$\frac{\partial \vec{j}(\vec{r}, t)}{\partial t} = \vec{P}[\rho(\vec{r}, t)], \tag{8b}$$

where $\vec{P}[\rho(\vec{r}, t)]$ is a three-component density functional. These equations are equivalent to TDSE and time-dependent Kohn–Sham (TDKS) equations at the exact level [23]. The functional form of $\vec{P}[\rho(\vec{r}, t)]$ has been approximated [24] by taking a cue from

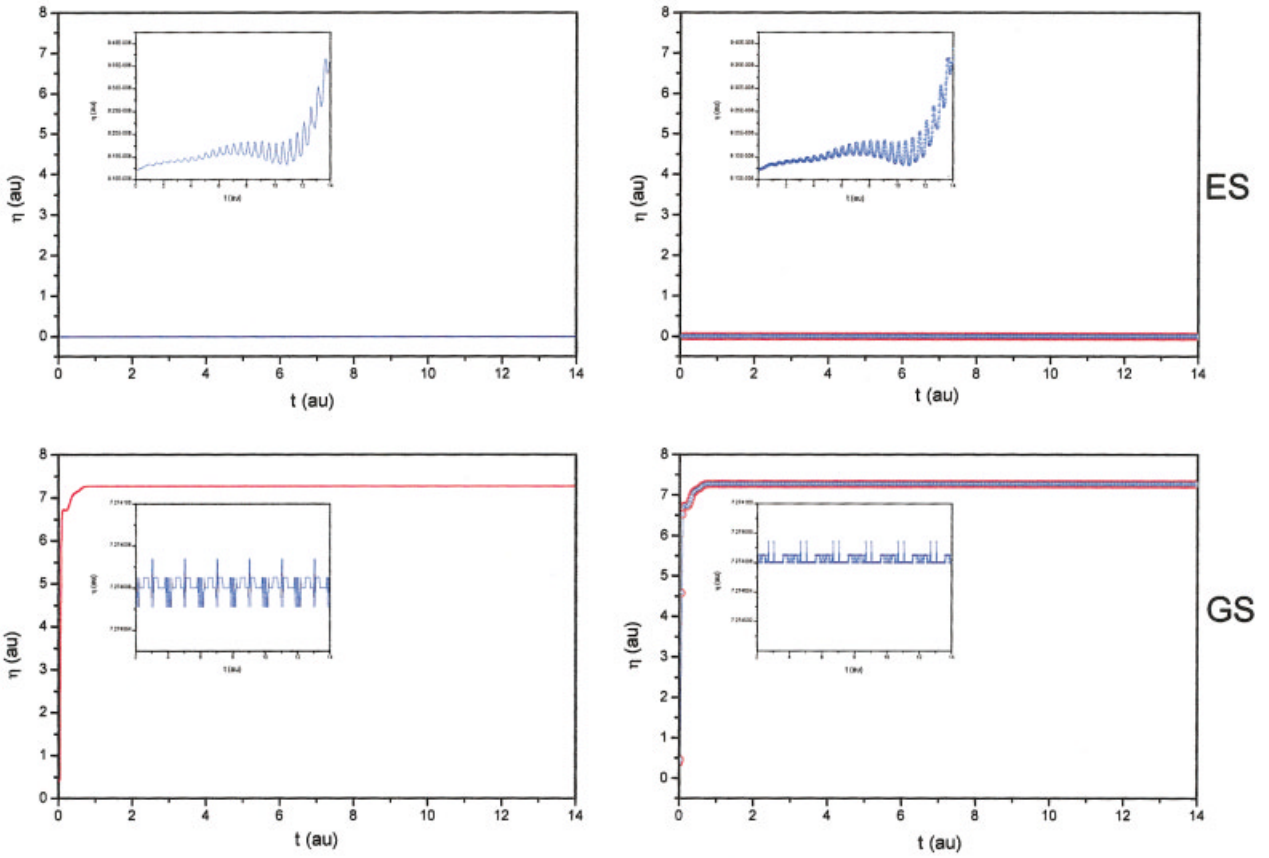

FIGURE 5. Time evolution of chemical hardness (η, a.u.) when a helium atom is subjected to external electric fields. See the caption of Fig. 3 for details.

DFT and this scheme is termed quantum fluid DFT (QFDFT). To know $\rho(\vec{r}, t)$ and $\vec{j}(\vec{r}, t)$ of a dynamic system at all times, QFDFT [24] is used. The overall dynamics of the ground state of the helium atom is studied by solving the generalized nonlinear Schrödinger equation (GNLSE) [24] (in a.u.), obtained by eliminating ζ [$\vec{j} = \rho\nabla\zeta$] from Eq. (8), as follows:

$$\left[-\frac{1}{2}\nabla^2 + v_{\text{eff}}(\vec{r}, t)\right]\phi(\vec{r}, t) = i\frac{\partial\phi(\vec{r}, t)}{\partial t}; \quad i = \sqrt{-1} \tag{9a}$$

where

$$\phi(\vec{r}, t) = \rho^{1/2}\exp(i\zeta) \tag{9b}$$

and

$$j(\vec{r}, t) = [\phi_{re}\nabla\phi_{im} - \phi_{im}\nabla\phi_{re}] = \rho\nabla\zeta. \tag{9c}$$

ζ is the velocity potential.

The effective potential in equation (9a) is given by

$$v_{\text{eff}}(\vec{r}, t) = \frac{\delta T_{\text{NW}}}{\delta\rho} + \frac{\delta E_{\text{xc}}}{\delta\rho} + v2_{\text{core}}(\vec{r}) + \int\frac{\rho(\vec{r}, t)}{|\vec{r} - \vec{r}'|}d\vec{r}' + v_{\text{ext}}(\vec{r}, t), \tag{10}$$

where T_{NW} and E_{xc} denote the non-Weizsäcker part of the kinetic energy and exchange-correlation energy functionals, respectively, and $v2_{\text{core}}(\vec{r}) = -(2/r)$.

The non-Weizsäcker part [19] of the kinetic energy functional is given by

$$T_{\text{NW}} = C_k\int\rho^{5/3}d\vec{r} - a(N)\lambda\int\frac{\frac{\rho^{4/3}}{r}}{1 + \frac{r\rho^{1/3}}{0.043}}d\vec{r}, \tag{11}$$

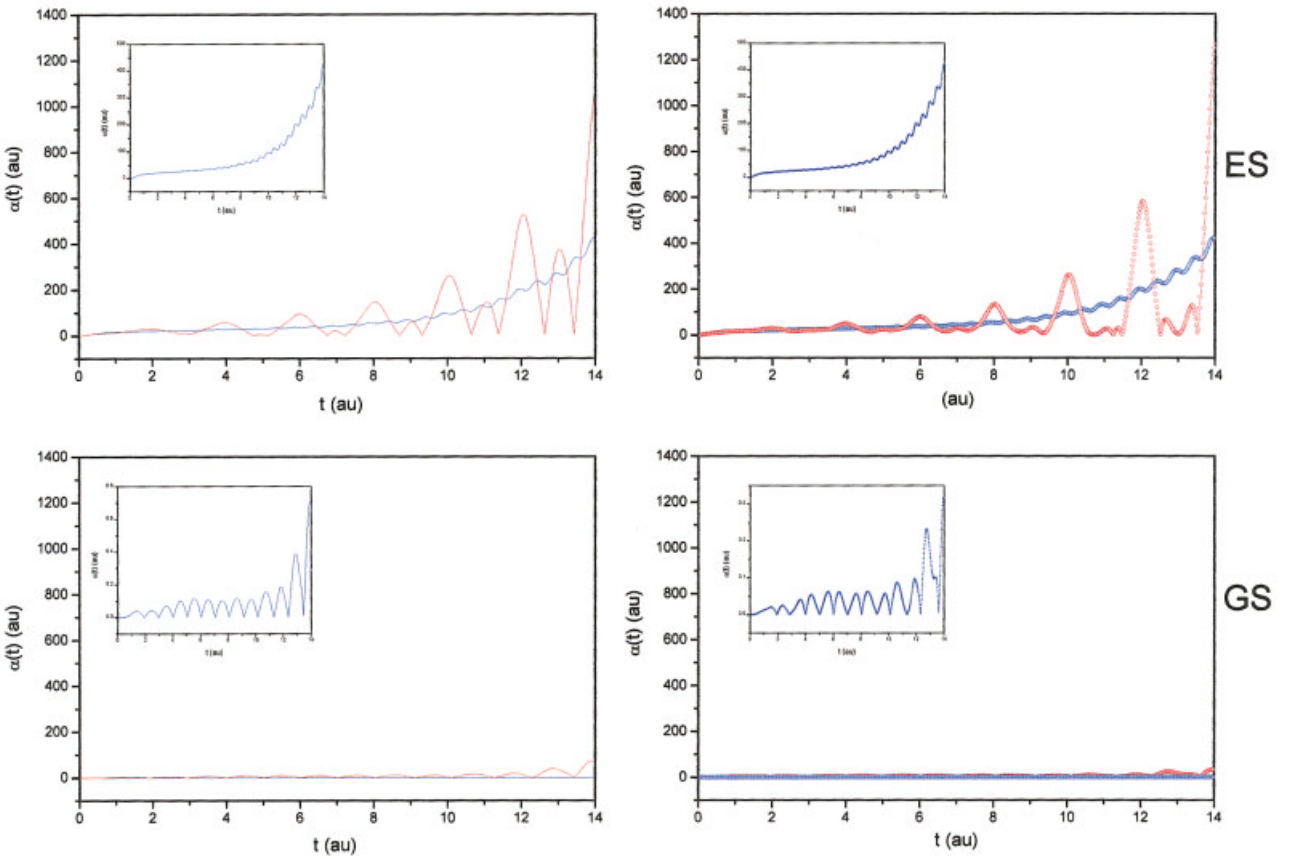

FIGURE 6. Time evolution of polarizability ($\alpha(t)$, a.u.) when a hydrogen atom is subjected to external electric fields. See the caption of Fig. 2 for details.

where $C_k = (3/10)(3\pi^2)^{2/3}$; $\lambda = 30(3/\pi)^{1/3}$; $a(N) = 0.1279 + 0.1811N^{-1/3} - 0.0819N^{-2/3}$ and the exchange-correlation is the sum of modified Dirac exchange functional $E_x[\rho]$ and the Wigner-type parameterized correlation energy function $E_c[\rho]$. It may be noted that this treatment is general and may be applied to systems (atoms and molecules) with more than two electrons as well. However, for a complete treatment vibrational and rotational degrees of freedom in addition to an electronic one are to be considered in the case of molecules.

We have taken $E_x[\rho]$ as [25]

$$E_x[\rho] = -C_x\left[\int \rho^{4/3} d\vec{r} + \int \frac{\rho^{4/3}}{1 + \dfrac{r^2\rho^{2/3}}{0.0244}}\, d\vec{r}\right], \quad (12)$$

where $C_x = (3/4\pi)(3\pi^2)^{1/3}$ and $E_c[\rho]$ as [26]

$$E_c[\rho] = -\int \frac{\rho}{9.81 + 21.437\rho^{-1/3}}\, d\vec{r}. \quad (13)$$

A time-dependent energy functional can be defined [23, 27, 28] as the following density functional:

$$E(t) = \frac{1}{2}\int \rho(\vec{r}, t)|\nabla\zeta|^2 d\vec{r} + T[\rho] + E_{xc}[\rho] + \int v_{\text{core}}(\vec{r})\rho(\vec{r}, t)d\vec{r} + \frac{1}{2}\iint \frac{\rho(\vec{r}, t)\rho(\vec{r}', t)}{|\vec{r} - \vec{r}'|}\, d\vec{r}d\vec{r}' + \int v_{\text{ext}}(\vec{r}, t)\rho(\vec{r}, t)d\vec{r}, \quad (14)$$

where $v_{\text{core}}(\vec{r}) = v1_{\text{core}}(\vec{r})$ for the hydrogen ground, excited, and helium excited states and $= v2_{\text{core}}(\vec{r})$ for the helium ground state.

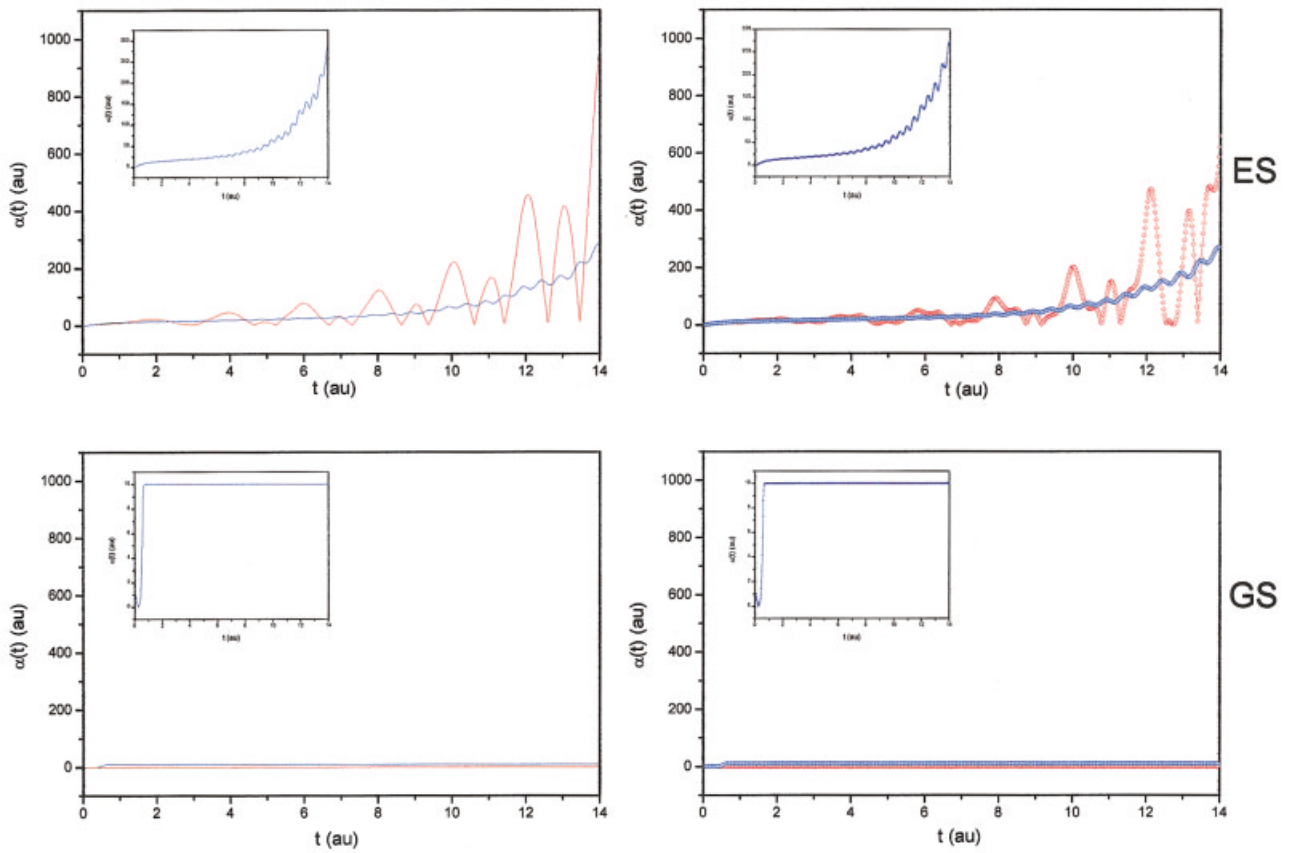

FIGURE 7. Time evolution of polarizability ($\alpha(t)$, a.u.) when a helium atom is subjected to external electric fields. See the caption of Fig. 3 for details.

Because chemical potential, μ, is the first-order functional derivative of the energy functional with respect to density (ρ), it may be defined as

$$\mu(t) = \frac{\delta E(t)}{\delta \rho} = \frac{1}{2}|\nabla \zeta|^2 + \frac{\delta T}{\delta \rho} + \frac{\delta E_{xc}}{\delta \rho} + v_{\text{core}}(\vec{r}) + \int \frac{\rho(\vec{r}, t)}{|\vec{r} - \vec{r}'|} d\vec{r}' + v_{\text{ext}}(\vec{r}, t). \quad (15)$$

Now, as the chemical potential becomes equal to the total electrostatic potential at a point $\vec{r}_c$ [29], we get

$$\mu(t) = -\chi(t) = v_{\text{core}}(\vec{r}) + \int \frac{\rho(\vec{r}, t)}{|\vec{r}_c - \vec{r}|} d\vec{r} + v_{\text{ext}}(\vec{r}_c, t), \quad (16)$$

where

$$\left[\frac{1}{2}\left|\nabla \zeta\right|^2 + \frac{\delta T}{\delta \rho} + \frac{\delta E_{xc}}{\delta \rho}\right]\Bigg|_{r=r_c} = 0. \quad (17)$$

Because the global hardness η depends on $f(\vec{r})$, $\eta(\vec{r}, \vec{r}')$, and $\rho(\vec{r})$ to obtain the global hardness η, we have to know the Fukui function $f(\vec{r})$ and the hardness kernel $\eta(\vec{r}, \vec{r}')$. The formula for $f(\vec{r})$ [13] is taken here as

$$f(\vec{r}) = \frac{s(\vec{r})}{\int s(\vec{r}) d\vec{r}}, \quad (18)$$

where $s(\vec{r})$ is the local softness given by [30]

$$s(\vec{r}) = \frac{\delta(\vec{r} - \vec{r}')}{2\eta(\vec{r}, \vec{r}')}. \quad (19)$$

For calculating the hardness kernel $\eta(\vec{r}, \vec{r}')$, the following local form [19] for $F[\rho]$ is used

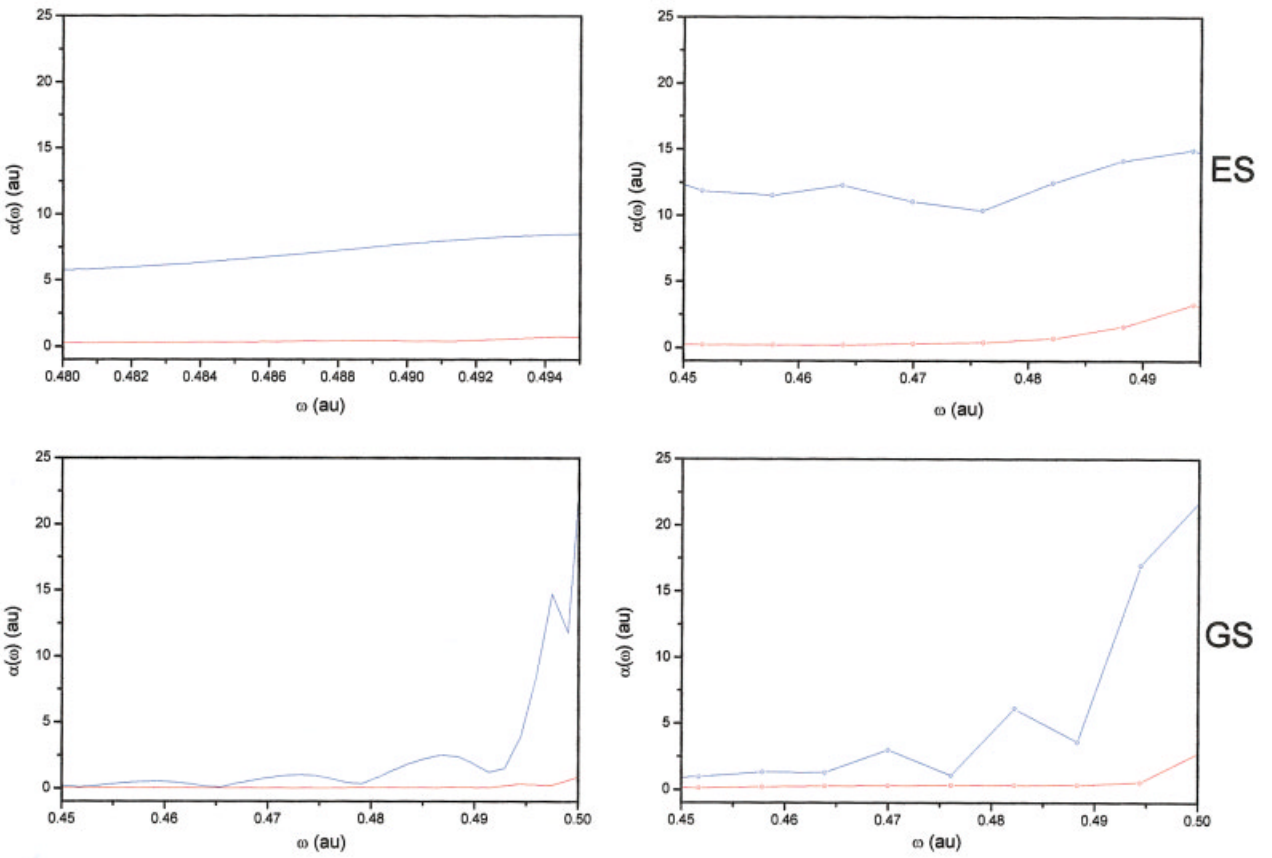

FIGURE 8. Plot of frequency-dependent polarizability ($\alpha(\omega)$, a.u.) vs. ω when a hydrogen atom is subjected to external electric fields. See the caption of Fig. 2 for details.

$$F[\rho] = T^{\text{local}}[\rho] + V_{\text{ee}}^{\text{local}}[\rho] \tag{20}$$

where local kinetic energy [25] $T^{\text{local}}[\rho]$ and electron–electron repulsion energy [31] $V_{\text{ee}}^{\text{local}}[\rho]$ are taken as

$$T^{\text{local}}[\rho] = C_k \int \rho^{5/3} d\vec{r} + C_x \int \frac{\dfrac{\rho^{4/3}}{r}}{1 + \dfrac{r\rho^{1/3}}{0.043}} d\vec{r} \tag{21}$$

and

$$V_{ee}^{\text{local}}[\rho] = 0.7937(N-1)^{2/3} \int \rho^{4/3} d\vec{r}. \tag{22}$$

Because $N = 1$ for hydrogen atom, $V_{\text{ee}}^{\text{local}}[\rho] = 0$ for this case.

To follow the polarizability dynamics the diagonal z-component of the time-dependent dipole polarizability tensor is written as

$$\alpha(t) = \frac{|D_{\text{ind}}^{z}(t)|}{\varepsilon_0}, \tag{23}$$

where $D_{\text{ind}}^{z}(t)$ is the z-component of the electronic part of the induced dipole moment and ε_0 is the maximum amplitude of the external field. It may be noted that an axial (z-direction) external electric field [Eq. (6)] is used in the present study. We also studied the behavior of the corresponding frequency-dependent quantity.

The phase volume or uncertainty product is an important diagnostic [16, 32] of the quantum signature of classical chaos, as it is related to the compactness of the electron cloud [33]. For the present case it may be defined in cylindrical polar coordinate ($\tilde{\rho}, \tilde{z}, \phi$) as

$$V_{ps} = \{\langle (p_{\tilde{\rho}} - \langle p_{\tilde{\rho}} \rangle)^2 \rangle \langle (p_{\tilde{z}} - \langle p_{\tilde{z}} \rangle)^2 \rangle \times \langle (\tilde{\rho} - \langle \tilde{\rho} \rangle)^2 \rangle \langle (\tilde{z} - \langle \tilde{z} \rangle)^2 \rangle\}^{1/2}. \tag{24}$$

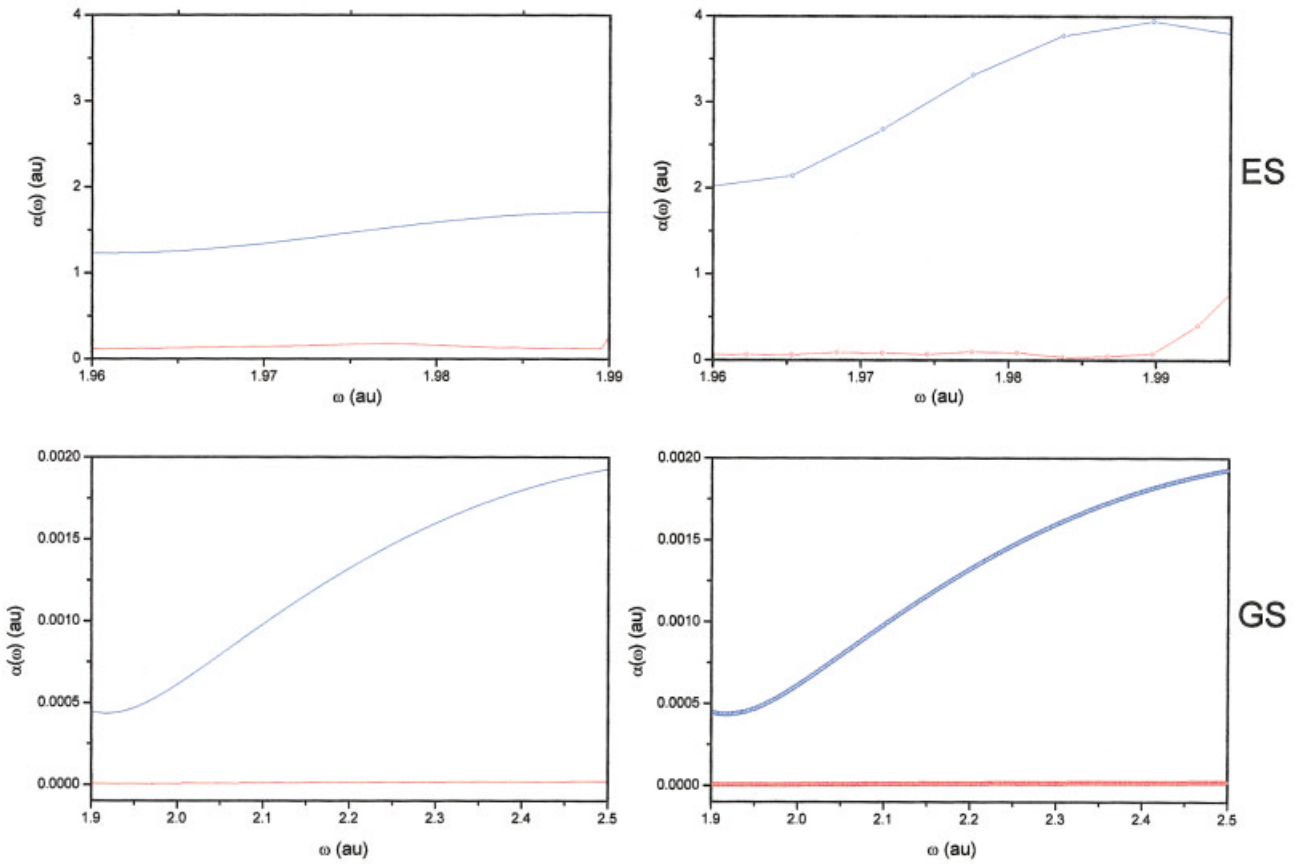

FIGURE 9. Plot of frequency-dependent polarizability ($\alpha(\omega)$, a.u.) vs. ω when a helium atom is subjected to external electric fields. See the caption of Fig. 3 for details.

A sharp increase in phase volume indicates a chaotic motion [32] because it is a measure of associated quantum fluctuations [32].

The electrophilicity index (w) is defined as [34]

$$w = \frac{\mu^2}{2\eta}, \tag{25}$$

which measures the propensity to absorb electrons.

It is known [35] that the experimental harmonic distribution is proportional to $|d(\omega)|^2$, where $d(\omega)$ is the Fourier transform of the induced dipole moment.

3. Numerical Details

For the hydrogen ground and excited states and the helium excited state we numerically solve the TDSE. It is an initial boundary value problem and is solved using an alternating direction implicit method [36]. Because the electron density is varying along the $\tilde{\rho}$ axis, we make the transformation

$$y = \tilde{\rho}\psi \tag{26}$$

and

$$\tilde{\rho} = x^2. \tag{27}$$

After this transformation the TDSE takes the following form in the transformed variables (after the analytic integration is carried out over $0 \le \phi \le 2\pi$):

$$\left\{\left(\frac{3}{4x^3}\right)\frac{\partial y}{\partial x} - \left(\frac{1}{4x^2}\right)\frac{\partial^2 y}{\partial x^2} - \frac{\partial^2 y}{\partial \tilde{z}^2}\right\} - \left(\frac{1}{x^4} - 2(v_{\text{core}} + v_{\text{ext}})\right)y = 2i\frac{\partial y}{\partial t}. \tag{28}$$

The numerical solution proceeds with ψ_{1s} and ψ_{15s} for H. For He, a properly normalized hydrogenic 15s-type wave function is taken at $t = 0$. The

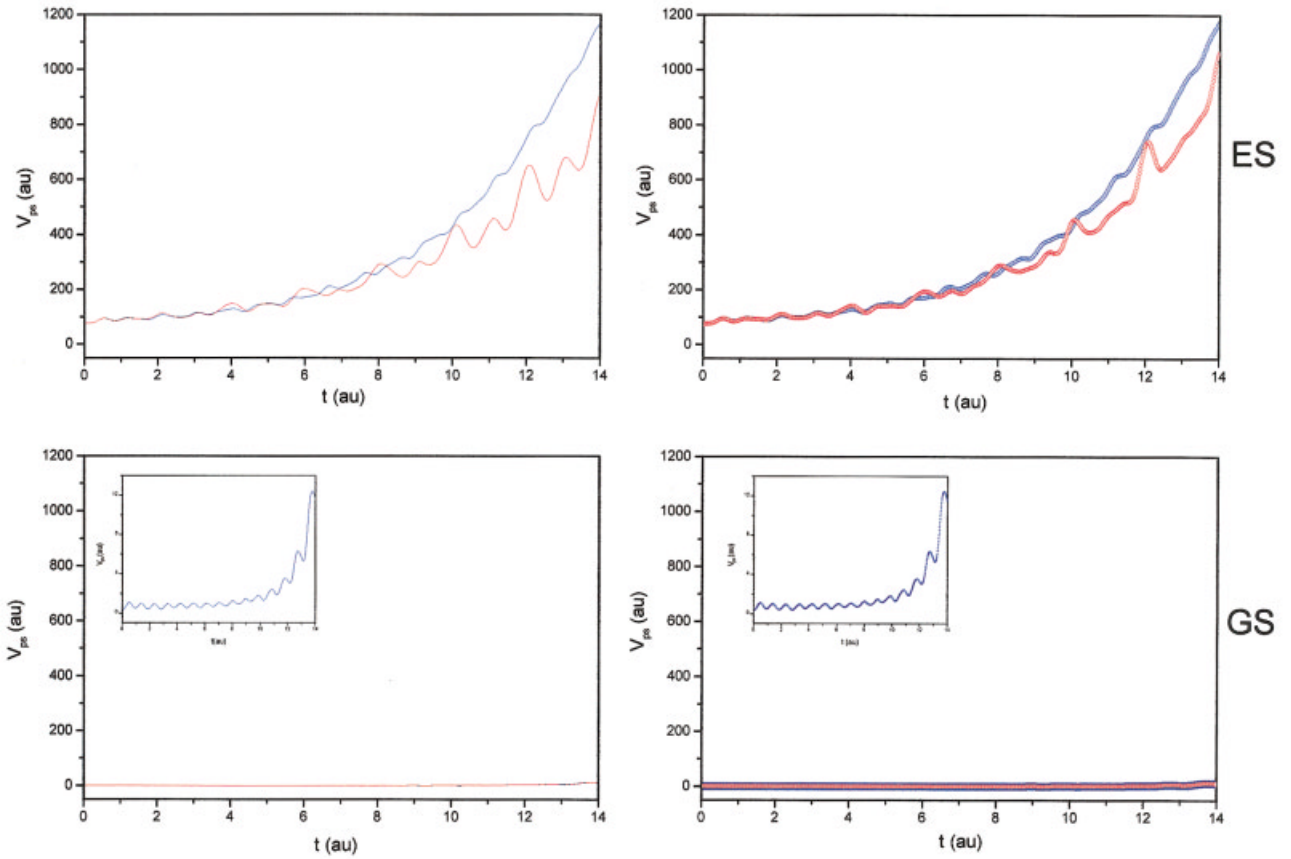

FIGURE 10. Time evolution of phase volume (V_{ps}, a.u.) when a hydrogen atom is subjected to external electric fields. See the caption of Fig. 2 for details.

resulting tridiagonal matrix equation is solved using Thomas' algorithm. The mesh sizes adopted here are $\Delta x = \Delta z = 0.4$ a.u. and $\Delta t = 0.01$ a.u. The forward-time-central-space type numerical scheme is used here.

The initial and boundary conditions associated with this problem are

$$y(x, \tilde{z}) \text{ is known} \qquad \forall\, x, \tilde{z} \text{ at } t = 0 \qquad (29a)$$

$$y(0, \tilde{z}) = 0 = y(\infty, \tilde{z}) \qquad \forall\ \tilde{z}, t \qquad (29b)$$

$$y(x, \pm\infty) = 0 \qquad \forall\, x, t \qquad (29c)$$

The numerical scheme is stable [37] because of the presence of $i = \sqrt{-1}$. We have verified the conservation of the norm and energy (in zero field case) as well. Calculations are done in double precision. The parameters are taken as $\varepsilon_0 = 0.01$ and 1, $t = 14$, and $\omega_0 = \pi$ and $\omega_1 = 2\omega_0$ (all are in atomic units). The intensity corresponding to these field amplitudes are, respectively, 3.509×10^{12} and 3.509×10^{16} W/cm^2. These intensity values are chosen because such pulses can overcome the force experienced by an electron in the first Bohr orbit by the static nuclear Coulomb field [22] and optical harmonic generation [38] and multiphoton ionization [22] take place for the short laser pulses of high intensity like this.

To study the helium ground state, the GNLSE is solved with a near-Hartree–Fock ground-state density of He. For the GNLSE we adopt a leapfrog-type finite difference scheme [36] with the rest of the quantities remaining the same. A different mesh structure is used in this case viz. $\Delta x = \Delta z = 0.05$ and $\Delta t = 0.0125$.

4. Results and Discussion

The time dependence of various quantities are depicted in figures 1–15. GS and ES, respectively, refer to the ground and excited electronic states of the systems whereas blue and red refer to two different intensities, viz. 3.509×10^{12} and 3.509×10^{16} W/cm^2, respectively, for hydrogen and helium unless otherwise specified. It may be noted that

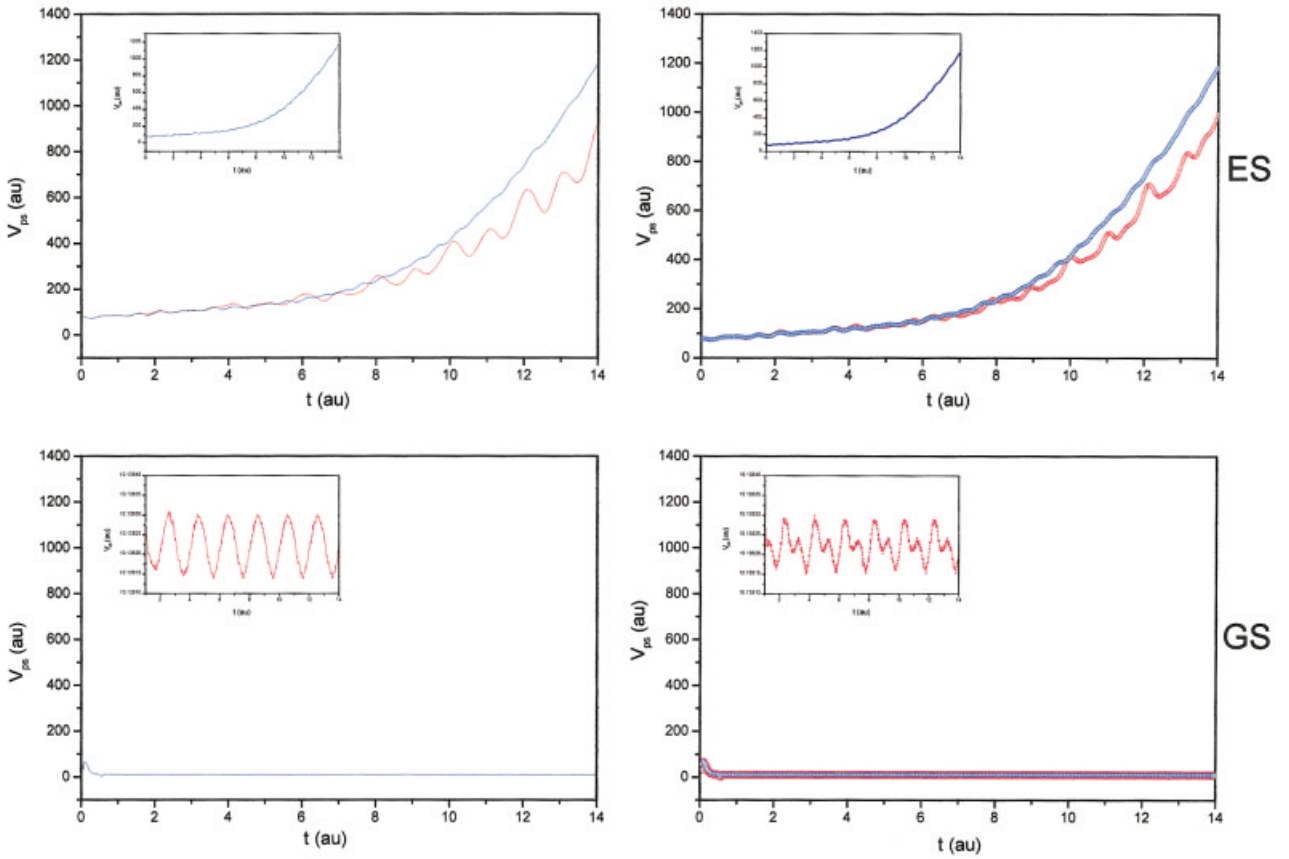

FIGURE 11. Time evolution of phase volume (V_{ps}, a.u.) when a helium atom is subjected to external electric fields. See the caption of Fig. 3 for details.

these colors have nothing to do with the two different frequencies (hence colors) used in the present calculation. A solid line and a dot-centered line, respectively, signify monochromatic and bichromatic pulses. In most cases the lower-intensity plots are zoomed in the inset. Atomic units are used throughout.

Figure 1 presents the time dependence of the external electric field with different amplitudes and frequencies. This quantity is presented to show the different types of in-phase and out-of-phase oscillations of various reactivity parameters as the systems evolve in course of time in the presence of external field.

Figures 2 and 3 present the time evolution of chemical potential (μ) for hydrogen and helium, respectively. The magnitude of chemical potential for the ground state of hydrogen is higher than that of the excited state of hydrogen, but for the ground state of helium it is lower than that of the excited state of helium. Now, comparing the ground states of hydrogen and helium, we see that the chemical potential of the hydrogen ground state is much more than the helium ground state. For the helium ground state there is a clear-cut oscillation in μ which is in-phase with the external field for both the monochromatic and bichromatic pulses and for both the intensities (lower-intensity plot is zoomed in the inset). An apparent in-phase oscillation is discernible for the envelope of the μ-profile of the hydrogen ground state, which is more conspicuous for the external field of larger intensity. However, there is no clear-cut in-phase oscillation for either of the excited states. As soon as the external electric field is switched on, there starts a competition between the nuclear Coulomb field and the external electric field to govern the electron density distribution [39]. Owing to the central nature, the nuclear field tries to make the density spherically symmetrical with characteristic oscillations while the external axial field tries to make it cylindrically symmetrical. For the small amplitude of the external field the in-phase oscillation is not observed. Only when the strength of the external field is such that it dominates over the nuclear field we observe in-phase oscillations in reactivity index profiles. In

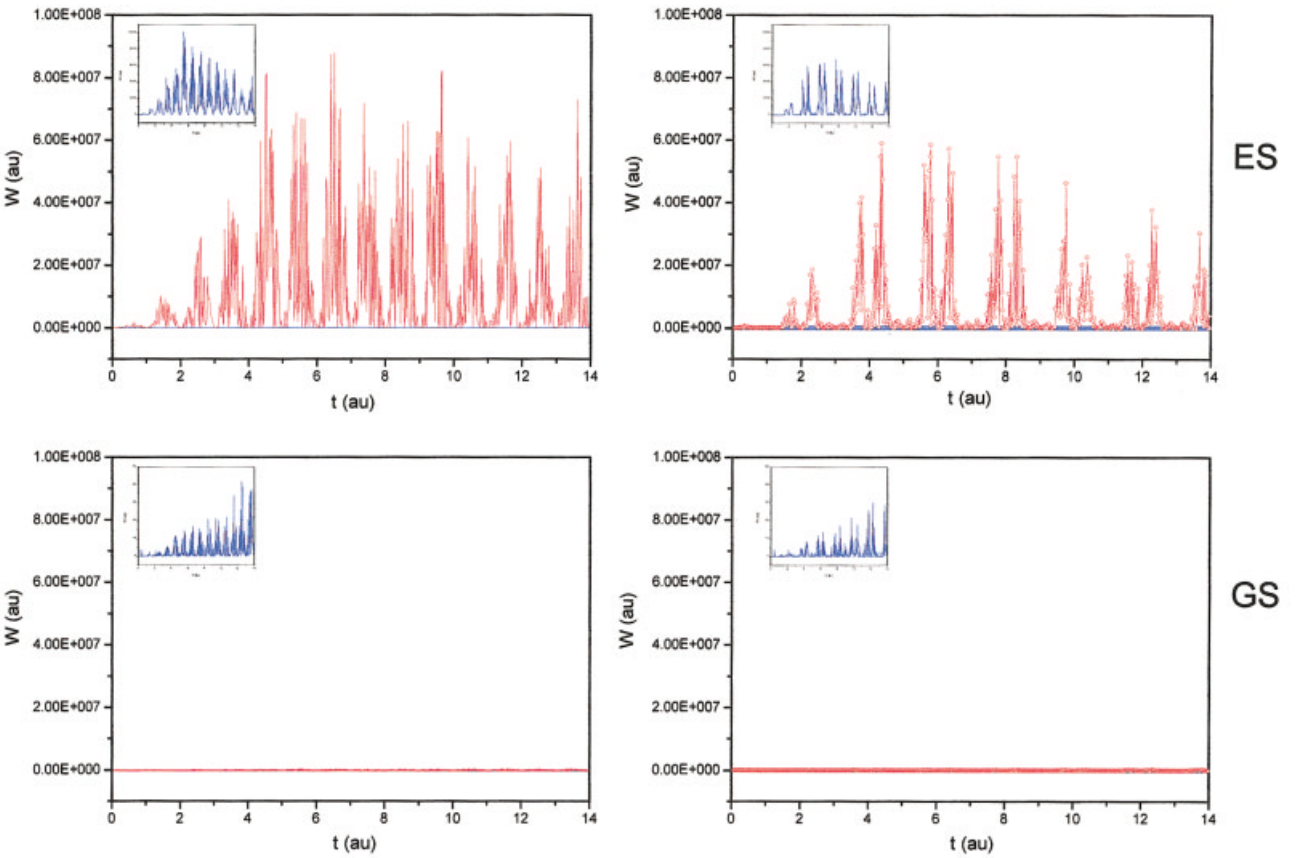

FIGURE 12. Time evolution of electrophilicity index (w, a.u.) when a hydrogen atom is subjected to external electric fields. See the caption of Fig. 2 for details.

that case, the frequency of oscillation in the profiles of reactivity indices matches with that of the external field. This in-phase oscillation in the dynamic μ-profile is a highly satisfactory feature considering the complicated roundabout way of the calculation of μ.

Time evolution of chemical hardness (η) for H and He are presented in Figures 4 and 5, respectively. For both hydrogen and helium atoms, chemical hardness in the ground state is higher than that of the excited state for both colors and intensities of the external field. If we compare the ground states of hydrogen and helium we can see that chemical hardness of helium is higher than that of hydrogen. According to the MHP the ground states of both H and He are more stable than the respective excited states vis-à-vis chaotic ionizations in these atoms. But, when we compare the excited states of hydrogen and helium the hydrogen excited state has higher chemical hardness than that of helium. This implies that the chaotic behavior in the helium excited state is more than that of the hydrogen excited state, which may be akin to the lower chaotic ionization threshold amplitude for helium in comparison to that of hydrogen. Unlike the μ-oscillations, although there are some oscillations in the η-profile it is neither in-phase nor steady throughout, which is conspicuous for the bichromatic case. It may be due to the fact that the first-order variation in energy due to external perturbation is significantly larger than the corresponding second-order one.

The time dependence of polarizability of H and He are, respectively, given in Figures 6 and 7 and the corresponding frequency-dependent quantities in Figures 8 and 9, respectively. The $\alpha(t)$ values for both the hydrogen and helium ground states are smaller than the corresponding excited state values, as would have been expected from MPP. The $\alpha(t)$ oscillations are also not in-phase with that of the external field. The frequency-dependent polarizability, $\alpha(\omega)$, for both the electronic states of H and He increases with ω as shown by others [40]. For both H and He the ground state $\alpha(\omega)$ is smaller than that in the excited state, a vindication of MPP.

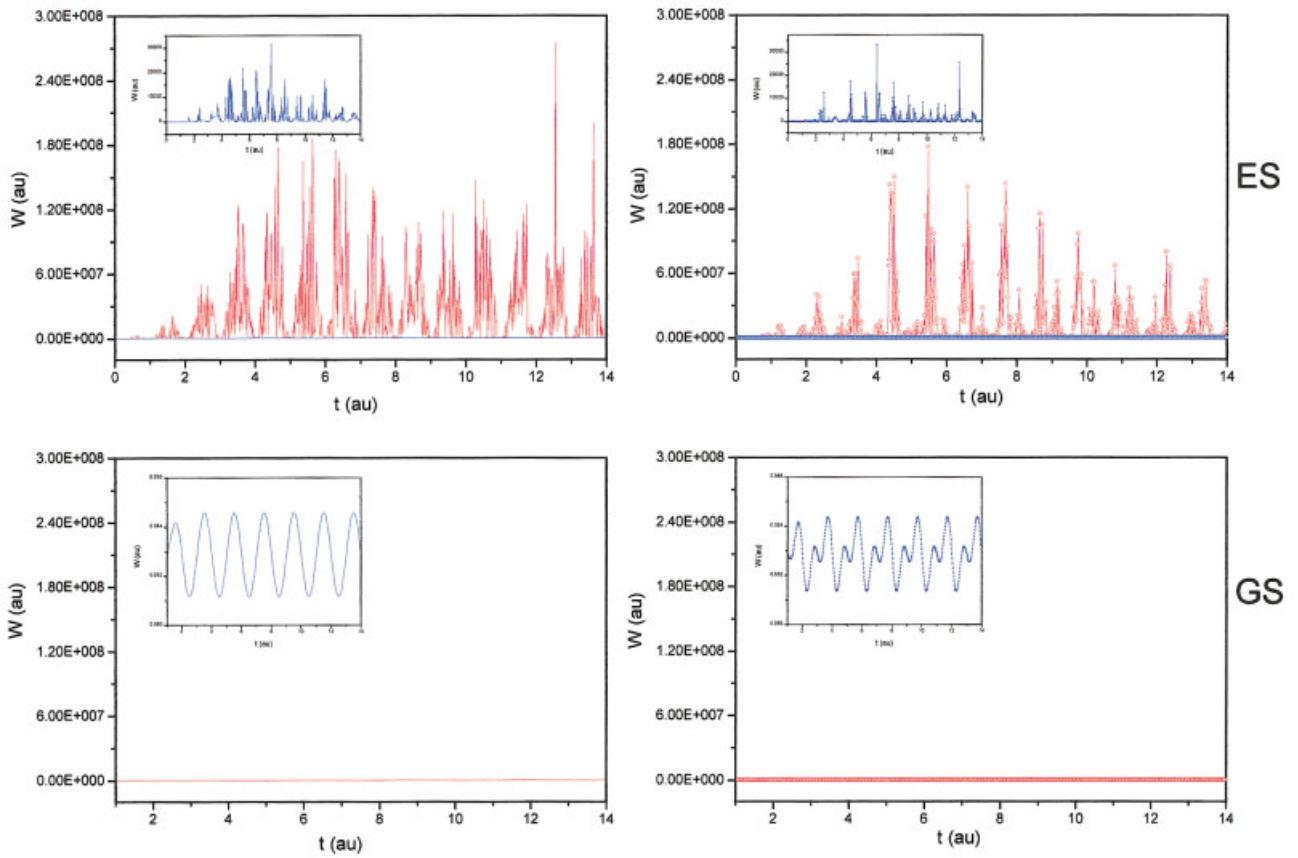

FIGURE 13. Time evolution of electrophilicity index (w, a.u.) when a helium atom is subjected to external electric fields. See the caption of Fig. 3 for details.

Figures 10 and 11 depict the dynamics of uncertainty product, V_{ps}, for H and He, respectively. In the ground state of hydrogen, the phase volume is slowly increasing and oscillating neither in-phase nor out-of-phase with the external field but for the excited state of hydrogen it is rapidly increasing and it also oscillates neither in-phase nor out-of-phase. In case of helium atom, the ground-state phase volume exhibits beautiful in-phase oscillation for both colors and both intensities are more pronounced for the more intense field (with zoomed inset for the field with the smaller amplitude in one-color pulse and with the larger amplitude in two-color pulse), whereas at excited state V_{ps} is increasing with its characteristic oscillations. Initially, the phase volume of the hydrogen ground state is lower than that of the helium ground state but finally it is higher than that of the latter. But, if we make comparison between the excited states of the two atoms they are nearly equal. This is because in the Rydberg state the helium atom behaves as a pseudo-one electron system. Large phase volume for the excited states discerns their chaotic behavior owing to larger quantum fluctuations in the less compact electron cloud in the phase space [5] in comparison to the regular ground-state dynamics.

Figures 12 and 13 represent the time dependence of electrophilicity index (w) for H and He, respectively. The ground-state electrophilicity index is lower in magnitude in comparison to the excited state electrophilicity index for both hydrogen and helium. Comparison between the ground and excited states of hydrogen and helium shows that the relative w values for hydrogen and helium depend on the field amplitude and the color. Beautiful in-phase oscillations in w are discernible for both the monochromatic and bichromatic laser pulses for the less intense field interacting with the ground electronic state of the helium atom.

An analysis of the dynamic profiles of chemical potential, hardness, and electrophilicity reveals that a low-intensity field is sufficient to cause in-phase oscillations in the case of the chemical potential and electrophilicity but for a similar effect in the case of the hardness a stronger field is necessary. Profiles of μ and w are supposed to mirror each other because

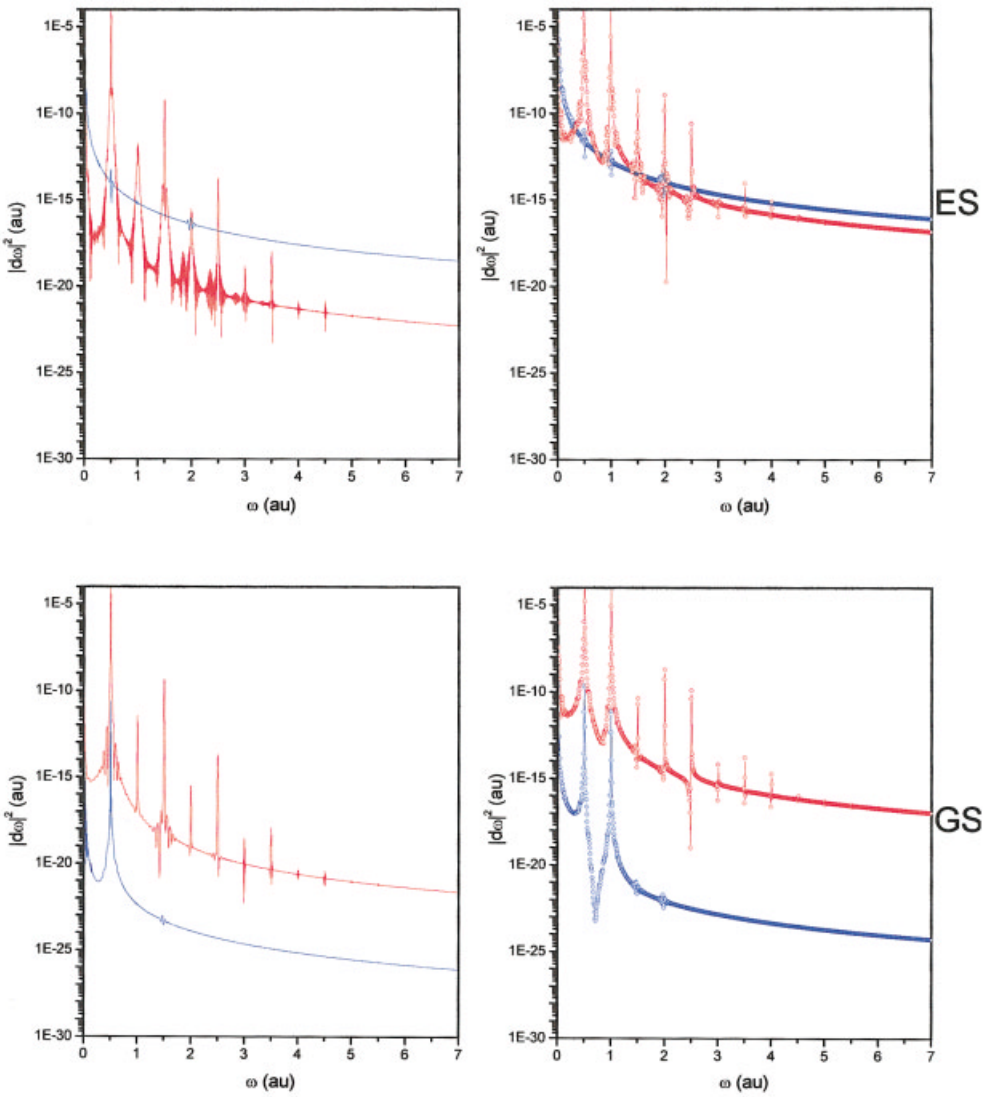

FIGURE 14. Harmonic spectra (a.u.) of hydrogen atom for various laser frequencies and intensities. See the caption of Fig. 2 for details.

electronegativity and electrophilicity ought to follow similar trends. In the present study we found this to be true. It is expected that a different choice of the functionals for the kinetic, exchange, and correlation energies would produce different numerical values of these reactivity indices. However, the qualitative features of the respective dynamic profiles will be similar.

Finally, the harmonic spectra are depicted in Figures 14 and 15 for H and He, respectively. Characteristic oscillations and eventual leveling off in these plots are observed. The envelopes of these figures resemble those reported by Erhard and Gross [41] and Krause et al. [38, 42], which is more pronounced when we repeat our calculations with their parameter values (not shown here). For both H and He, the more intense field generates more intense harmonics for most of the ω values and the harmonics generated by the bichromatic pulse is in general more intense than those that resulted from the monochromatic one. Harmonic intensity is in general smaller in the ground state than that in the excited state (but for H with more intense field where the values are more or less comparable), perhaps originating from the larger chaoticity of the highly excited states. These results are in conformity with other experimental [35, 43] and theoretical [38, 41, 42] results from the solutions of TDSE, TDKS, and TD Hartree–Fock equations as well as by using the solutions of TD-optimized effective

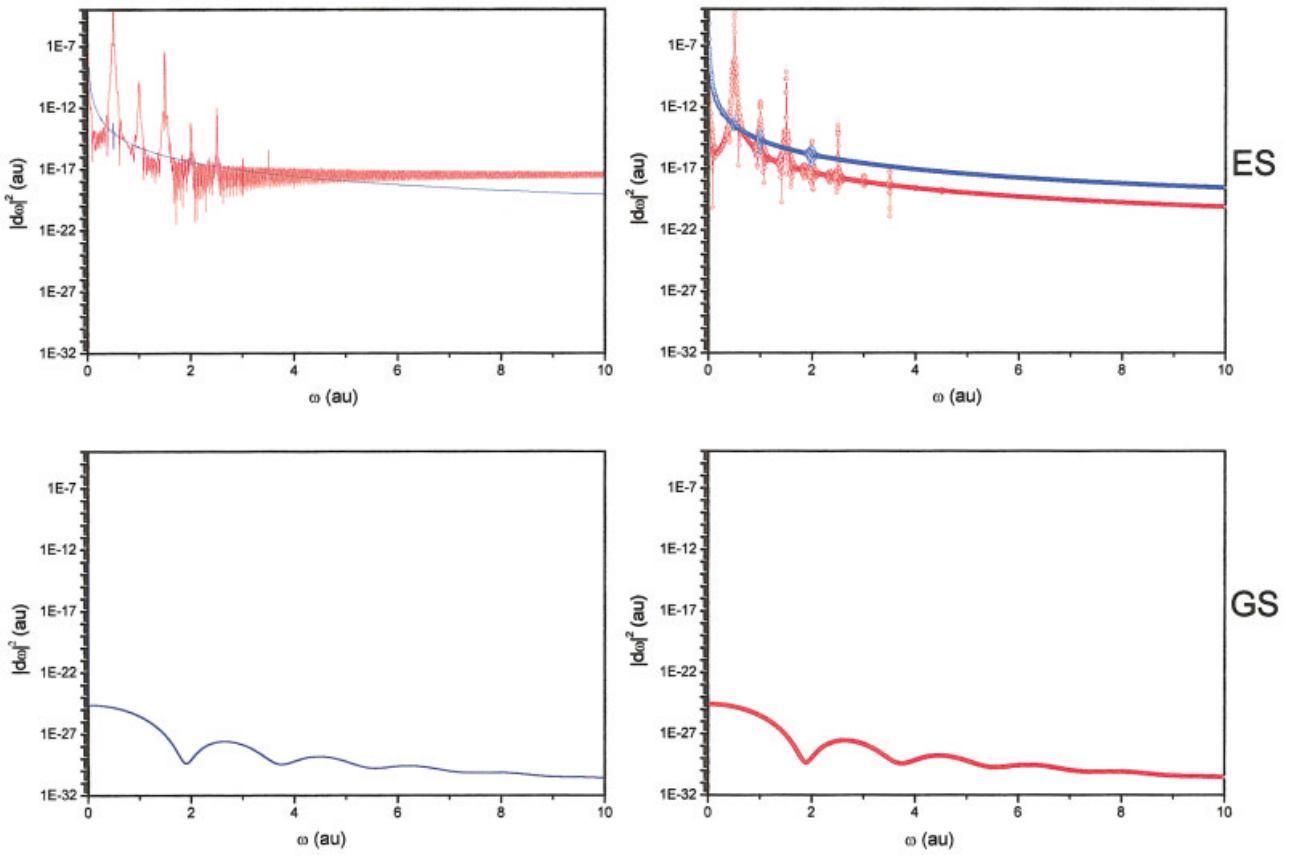

FIGURE 15. Harmonic spectra (a.u.) of helium atom for various laser frequencies and intensities. See the caption of Fig. 3 for details.

potential [44] and other methods [45]. A slight variation in details is due to the use of different parameters and different boundary conditions.

5. Conclusions

Dynamics of hydrogen and helium atoms in their ground and highly excited electronic states in the presence of *z*-polarized laser pulses of different colors and intensities are studied in terms of the time evolution of hardness, chemical potential, polarizability, phase volume, and electrophilicity index. The ground and excited states of hydrogen atom and the Rydberg state of helium atom are studied using time-dependent Schrödinger equations and the ground state of the helium atom is studied within a quantum fluid density functional framework. Dynamic variants of the principles of electronegativity equalization, maximum hardness, and minimum polarizability manifest themselves. A tug-of-war between the spherically symmetrical nuclear Coloumb field and cylindrically symmetrical external electric field to govern the electron density distribution is clearly delineated through the dynamic profiles of various reactivity indices for the monochromatic and bichromatic external fields of varying strengths.

In the ground state the hydrogen atom is harder and less polarizable with smaller phase volume, chemical potential, and electrophilicity index than the excited state. This also is the case of the helium atom. This means that in the ground state of hydrogen and helium both are more stable than the corresponding excited states. The ground-state helium atom is more stable than the ground-state hydrogen atom. However, the chaoticity of the excited state of helium is more than that of the excited state of hydrogen in the sense that it requires lower threshold amplitude for the chaotic ionization of helium than for that of hydrogen, which is in conformity with the corresponding experiment and the classical theory.

Harmonic spectra of the higher-order harmonics included in the radiation emitted by the resulting oscillating dipole are analyzed. Intensities of these

harmonics are larger in the cases of two-color pulse, field of higher amplitude, and excited states for both hydrogen and helium when compared to the harmonic intensities associated with one-color pulse, field of smaller intensity, and ground states, respectively, may be due to more regular behavior of the ground states.

The present study improves the overall understanding of the atom-field interactions and provides important insights into the chaotic ionization through the dynamics of various reactivity indices. Moreover, it will help in designing newer experiments for generating higher-order harmonics of larger intensities.

ACKNOWLEDGMENTS

This article is dedicated to Professor B. M. Deb on his 60th birthday. The authors thank the referee for constructive criticism and CSIR, New Delhi, for financial support.

References

1. Bayfield, J. E.; Koch, P. M. Phys Rev Lett 1974, 33, 258.
2. Mariani, D. R.; van de Water, W.; Koch, P. M.; Bergeman, T. Phys Rev Lett 1983, 50, 1261.
3. Mariani, D. R. Ph.D. thesis. Yale University: New Haven, CT, 1983.
4. Van de Water, W.; Yoakum, S.; van Leeuwen, K. A. H.; Sauer, B. E.; Moorman, L.; Galvez, E. J.; Mariani, D. R.; Koch, P. M. Phys Rev A 1990, 42, 537.
5. Jensen, R. V.; Sanders, M. M. Am J Phys 1996, 64, 1013; Jensen, R. V.; Sanders, M. M. Am J Phys 1996, 64, 21.
6. Parr, R. G.; Yang, W. Density Functional Theory of Atoms and Molecules; Oxford University Press: Oxford, UK, 1989.
7. Sen, K. D.; Jorgenson, C. K. Electronegativity: Structure and Binding, Vol. 66; Springer-Verlag: Berlin, 1987.
8. Sen, K. D.; Mingos, D. M. P. Chemical Hardness: Structure and Binding, Vol. 80; Springer-Verlag: Berlin, 1993.
9. Pearson, R. G. Hard and Soft Acids and Bases; Dowden, Hutchinson and Ross: Stroudsberg, PA, 1973; Pearson, R. G. Coord Chem Rev 1990, 100, 403.
10. Parr, R. G.; Donnelly, D. A.; Levy, M.; Palke, W. E. J Chem Phys 1978, 68, 3801.
11. Parr, R. G.; Pearson, R. G. J Am Chem Soc 1983, 105, 7512.
12. Berkowitz, M.; Ghosh, S. K.; Parr, R. G. J Am Chem Soc 1985, 107, 6811; Ghosh, S. K.; Berkowitz, M. J Chem Phys 1985, 83, 2976.
13. Parr, R. G.; Yang, W. J Am Chem Soc 1984, 106, 4049.
14. Pearson, R. G. J Chem Educ 1987, 64, 561; Pearson, R. G. Acc Chem Res 1993, 26, 250.
15. Sanderson, R. T. Science 1951, 114, 670; Sanderson, R. T. Science 1955, 121, 207; Sanderson, R. T. J Chem Educ 1954, 31, 238.
16. Chattaraj, P. K.; Sengupta, S. J Phys Chem A 1999, 103, 6122.
17. Chattaraj, P. K.; Sengupta, S. J Phys Chem 1996, 100, 16126.
18. Ghanty, T. K.; Ghosh, S. K. J Phys Chem 1996, 100, 12295.
19. Chattaraj, P. K.; Sengupta, S. J Phys Chem 1997, 101, 7893.
20. Chattaraj, P. K.; Poddar, A. J Phys Chem A 1998, 102, 9944; Chattaraj, P. K.; Poddar, A. J Phys Chem A 1999, 103, 1274; Chattaraj, P. K.; Fuentealba, P.; Gomez, B.; Contreas, R. J Am Chem Soc 2000, 122, 348; Fuentealba, P.; Simon-Manso, Y.; Chattaraj, P. K. J Phys Chem A 2000, 104, 3185; Chattaraj, P. K.; Fuentealba, P.; Jaque, P.; Toro-Labbe, A. J Phys Chem A 1999, 103, 9307.
21. Bethe, H. Handbuch der Physik, Vol. 24; Springer-Verlag: Berlin, 1933; p. 342.
22. Petersilka, M.; Gross, E. K. U. Laser Phys 1999, 9, 1; Kulander, K. C. Phys Rev A 1987, 35, 445.
23. Runge, E.; Gross, E. K. U. Phys Rev Lett 1984, 52, 997; Dhara, A. K.; Ghosh, S. K. Phys Rev A 1987, 35, 442.
24. Deb, B. M.; Chattaraj, P. K. Phys Rev A 1989, 39, 1696.
25. Ghosh, S. K.; Deb, B. M. J Phys B 1994, 27, 381.
26. Brual, G.; Rothstein, S. M. J Chem Phys 1978, 69, 1177.
27. Madelung, E. Z Phys 1926, 40, 322.
28. Deb, B. M.; Ghosh, S. K. J Chem Phys 1982, 77, 342; Bartolotti, L. J Phys Rev A 1982, 26, 2243.
29. Politzer, P.; Parr, R. G.; Murphy, D. R. J Chem Phys 1983, 79, 3859.
30. Fuentealba, P. J Chem Phys 1995, 103, 6571.
31. Parr, R. G. J Phys Chem 1988, 92, 3060.
32. (a) Feit, M. D.; Fleck, J. A. Jr. J Chem Phys 1984, 80, 2578; (b) Choudhury, S.; Gangopadhayay, G.; Ray, D. S. Ind J Phys 1995, 69B, 507; (c) Graham, R.; Hohnerbach, M. Phys Rev A 1991, 43, 3966; (d) Graham, R.; Hohnerbach, M. Phys Rev Lett 1990, 64, 637.
33. Pearson, R. G. Chemical Hardness: Application from Molecule to Solids; Wiley-VCH Verlag GMBH: Weinheim, Germany, 1997; p. 116.
34. Parr, R. G.; Szentpaly, L. v.; Liu, S. J Am Chem Soc 1999, 121, 1922.
35. Preston, S. G.; Sanpera, A.; Zepf, M.; Blyth, W. J.; Smith, C. G.; Wark, J. S.; Key, M. H.; Burnett, K.; Nakai, M.; Neely, D.; Offenberger, A. A. Phys Rev A 1996, 53, R31; L'Huillier, A.; Lompre, L. A.; Mainfray, G.; Manus, C. In: Gavrila, M., Ed. Atoms in Intense Laser Fields; Academic Press: Boston, 1992; p. 139; L'Huillier, A.; Balcou, P. Phys Rev Lett 1993, 70, 774.
36. Ames, W. F. Numerical Methods for Partial Differential Equations; Academic Press: New York, 1977, pp. 252.
37. Chattaraj, P. K.; Rao, K. S.; Deb, B. M. J Comput Phys 1987, 72, 504.
38. Krause, J. L.; Schafer, K. J.; Kulander, K. C. Phys Rev Lett 1992, 68, 3535.
39. Chattaraj, P. K. Int J Quantum Chem 1992, 41, 845; Dey, B. K.; Deb, B. M. Int J Quantum Chem 1995, 56, 707; Chattaraj, P. K.; Maiti, B. J Phys Chem A 2001, 105, 169.
40. Rérat, M.; Mérawa, M.; Pouchan, C. Phys Rev A 1992, 45, 6263, and references therein.
41. Erhard, S.; Gross, E. K. U. In: Lambropoulos, P.; Walther, H., Eds. Multiphoton Processes; IOP Publishing: London, 1997; pp. 37–45 and references therein.

42. Krause, J. L.; Schafer, K. J.; Kulander, K. C. Phys Rev A 1992, 45, 4998.
43. Watanabe, S.; Kondo, K.; Nabekawa, Y.; Sagisaka, A.; Kobayashi, Y. Phys Rev Lett 1994, 74, 2692; Eichmann, H.; Egbert, A.; Nolte, S.; Momma, C.; Wellegehausen, B.; Becker, W.; Long, S.; McIver, J. K. Phys Rev A 1995, 51, R3414.
44. Tong, X. M.; Chu, S. I. Phys Rev A 1998, 57, 452.
45. Schafer, K. J.; Kulander, K. C. Phys Rev A 1992, 45, 8026; Schafer, K. J.; Kulander, K. C. Phys Rev Lett 1997, 78, 638; Long, S.; Becker, W.; McIver, J. K. Phys Rev A 1995, 52, 2262; Protopapas, M.; Sanpera, A.; Knight, P. L.; Burnett, K. Phys Rev A 1995, 52, R2527.